

# Magnetic Properties of Nanoparticle $\text{Cu}_x\text{Co}_{1-x}\text{Fe}_{2-2y}\text{Al}_{2y}\text{O}_4$ Ferrite System

S. S. Karande<sup>1</sup>, B. R. Karche<sup>2</sup>

<sup>1</sup>Research scholars, JJT University, Jhunjhunu, Rajasthan, India

<sup>2</sup>Material Science and Thin Film Research Laboratory, Shankarrao Mohite Mahavidyalaya, Akluj (M.S) – 413101, India

**Abstract:** Samples of  $\text{Cu}_x\text{Co}_{1-x}\text{Fe}_{2-2y}\text{Al}_{2y}\text{O}_4$  ferrite system (where  $x= 0.0, 0.2, 0.4, 0.6, 0.8, 1.0$ ;  $y = 0.05, 0.15$  and  $0.25$ ) have been prepared by standard ceramic technique. Prepared samples are characterized by XRD, IR and SEM. Estimated particle size is found in the nanoparticle range. The effect of aluminum and copper on structural properties is studied. Magnetic properties of the samples are investigated by using Vibrating Sample Magnetometer (VSM) and Helmholtz's double coil apparatus. Addition of  $\text{Al}^{3+}$  replaces  $\text{Fe}^{3+}$  on A-site and hence magnetic moment per unit values decreases. Magnetic susceptibility decreases with aluminum and copper content. The initial permeability decreases with increase in frequency. Curie temperature of samples goes on decreases with addition of aluminum and copper in the host lattice of ferrite system. Copper cobalt ferrite exhibits canting of spins of magnetic moments on B-site. The canting angle  $\alpha_{yk}$  is found decreasing with  $\text{Al}^{3+}$  content in the host lattice.

**Keywords:** Polycrystalline copper cobalt ferrite, Magnetic moment, magnetic susceptibility, initial permeability, Coercive field, Saturation magnetization, canting angle ( $\alpha_{yk}$ ) and Curie temperature

## 1. Introduction

In a way, every material utilized today is a composite. Composite materials are a physical mixture of two or more compatible micro or macro constituent particles which differ in form and chemical composition and are essentially insoluble in each other. Composite materials are best suited for scientific applications which could not be achieved by any one component acting on its' own. Ferrite/ferroelectric composites are termed as magneto electric (ME) composites due to the coupling between the electric and magnetic fields in the materials. The conversion of magnetic to electric fields in such ME composite originates from the elastic interaction between ferrite and ferroelectric subsystems [1]. In the presence of the magnetic field, the magnetostriction in the ferrite phase gives rise to mechanical stresses that are transferred to the ferroelectric phase, resulting in electric polarization of the ferroelectric phase owing to its magneto electric effect. ME materials find applications as smart materials in actuators, sensors, magnetic probes, phase inverters, rectifiers, modulators, and transducers in solid state microelectronics and microwave devices [2,3].

Spinel ferrite nanoparticles are being intensively investigated in recent years because of their remarkable electrical and magnetic properties and wide practical applications in information storage system, Ferro-fluid technology, magneto caloric refrigeration and medical diagnosis [4]. Among the spinels, mixed Zn ferrites and especially Ni–Zn ferrites are widely used in applications like transformer cores, chokes, coils; noise filters recording heads etc [5]. While Ni–Zn ferrite possesses higher resistivity and saturation magnetization, cobalt ferrite possesses high cubic magnetocrystalline anisotropy and hence high coercivity. The high coercivity is driven by large anisotropy of the cobalt ions due to its important spin orbit coupling. It is ferromagnetic with a Curie temperature ( $T_c$ ) around 520 °C, [6] and shows a relatively large magnetic hysteresis which

distinguishes it from rest of the spinels. The synthesis of ultra fine magnetic particles has been extensively investigated in recent years because of their potential applications in high density magnetic recording and magnetic fluids [7]. Among the current methods for synthesis of mixed ferrite the combustion reaction method stands out as an alternative and highly promising method for the synthesis of these ferrites [8]. Magnetic properties measured at room temperature by vibrating sample magnetometer (VSM) reveal an increase in saturation magnetization with increase in cobalt concentration[9].

## 2. Experimental: -

The ferrites with general chemical formula  $\text{Cu}_x\text{Co}_{1-x}\text{Fe}_{2-2y}\text{Al}_{2y}\text{O}_4$  (where  $x= 0.0, 0.2, 0.4, 0.6, 0.8, 1.0$ ;  $y = 0.05, 0.15$  and  $0.25$ ) were prepared by the standard ceramic technique using AR grade cobalt oxide, copper oxide, ferric oxide and aluminium oxide. The compositional weights of powders were mixed physically and blended in agate mortar in acetone medium. The final sintering process was carried at 1000°C for 48 hours. The slow cooled samples were heated at rate of 80 °C per hour. The pellets and toroids were formed by using respective steel die. A universal testing machine as well as Archimedes's method was applied for determining the physical properties of the samples. The formation of the cubic spinel structure of the samples prepared is confirmed by X- ray diffraction analysis. Saturation magnetization of each was carried out using high-field hysteresis loop tracer and A.C susceptibility of slow cooled powder ferrite samples was measured in the temperature range 300-800K on Helmholtz's double coil set up operating of 263 Hz with a constant field of 7 Oersted discussed previously [10]. The saturation magnetization ( $\sigma_s$ ), magnetic moment ( $n_B$ ) were determined from the magnetization study and presented by graphs. Curie temperature of samples was estimated by Loria Sinha method [11] and from AC susceptibility measurement.

### 3. Results and Discussion

The lattice constants 'a' and 'c' for all prepared samples are calculated by using prominent (311) XRD peak. The calculated and observed values of inter planer distance (d) are found in good agreement with each other for all reflections (Fig.1). The particle size (D) for all the ferrite samples is calculated by Debye Scherer formula, ionic site radii ( $R_A$ ,  $R_B$ ) and ionic bond lengths (A-O, B-O) are calculated from the formulae given by Gadkari et.al [8] and presented in (Fig 2). From the calculations of lattice constants 'a' and 'c' for all the prepared ferrites it is observed that  $c > a$  and tetragonality ratio (c/a) is found in the range of 1.03 to 1.07. This result is in good agreement with previous report [12-13].

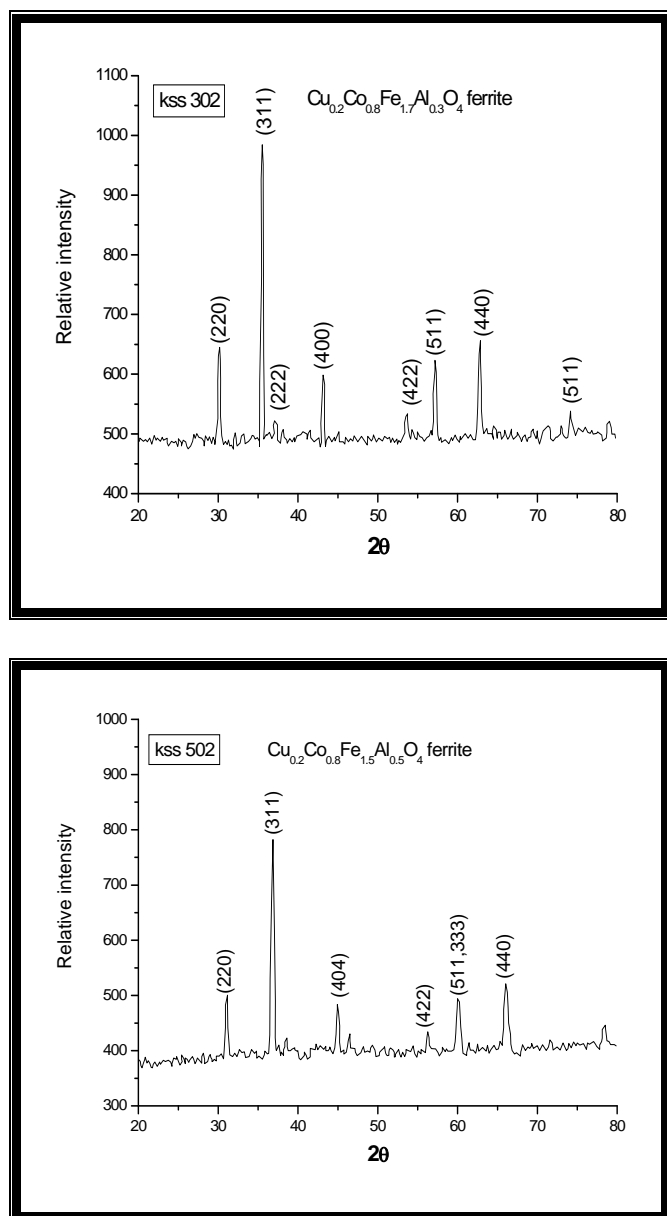
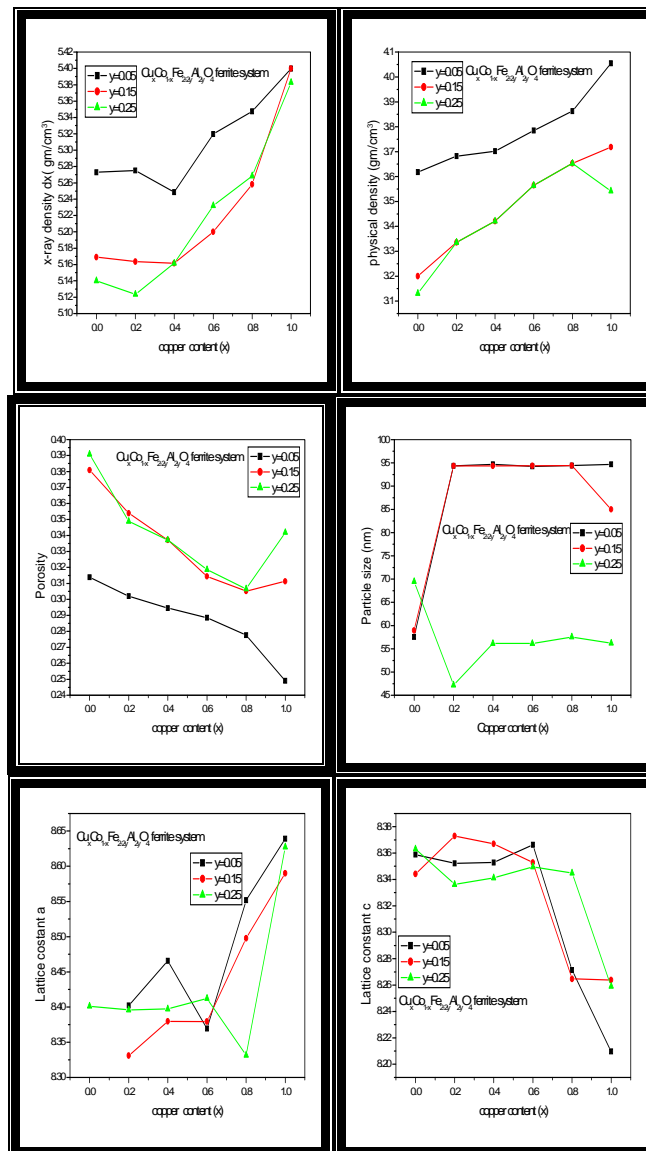
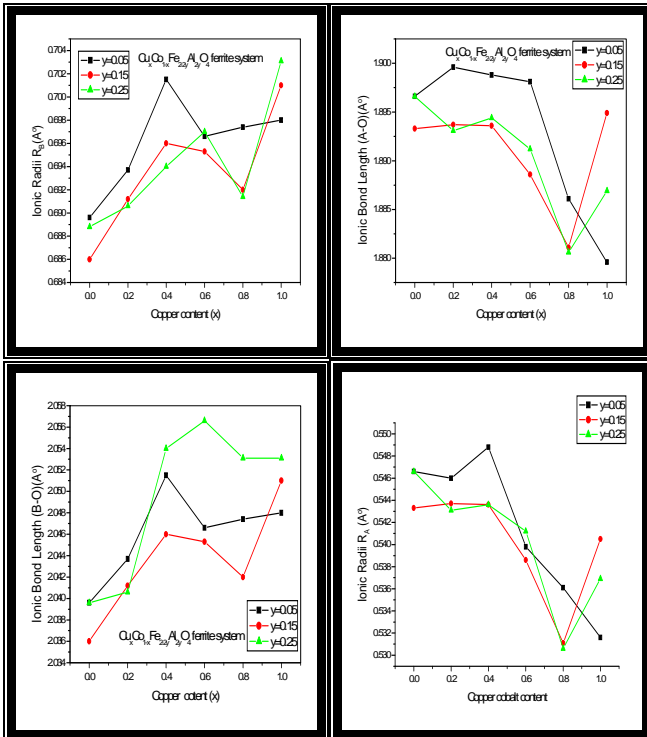


Figure 1: XRD patterns

The variation of tetrahedral metal oxygen bond length (A-O) and tetrahedral cationic radius  $R_A$  decrease with increase of copper as well as aluminum content which suggest the occupancy of  $Cu^{2+}$  ions at B site only. However, no considerable change in the values of octahedral metal

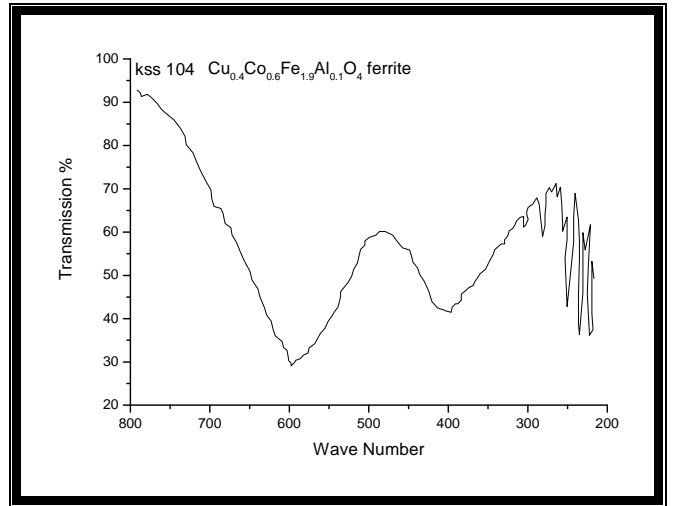
oxygen bond length (B-O) and octahedral cationic radius ( $R_B$ ) are observed. This could be due to the fact that increase in  $Cu^{2+}$  occupancy at B site replaces  $Fe^{3+}$ . The bond length B-O in all the compositions is found to be greater than bond length A-O. This is rather a normal behavior of spinel ferrites





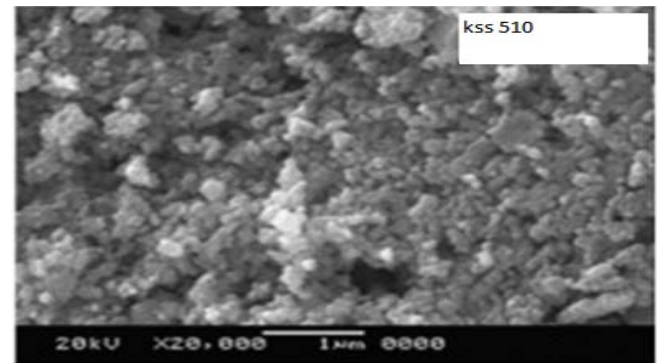
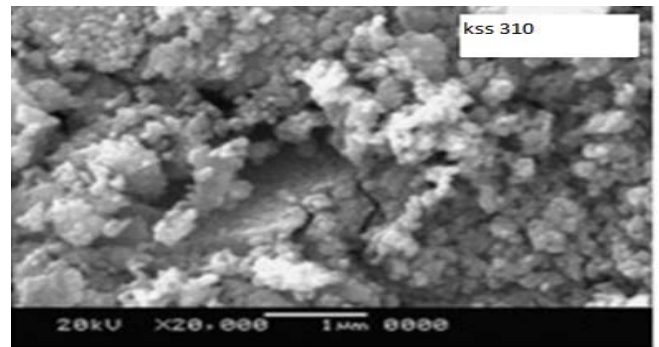
**Figure 2:** Variation of lattice constant a, lattice constant c, x-ray density, physical density, porosity, particle size, ionic radii  $R_A$ , ionic radii  $R_B$ , ionic bond length(A-O), ionic bond length(B-O) with copper content and aluminum content.

The infrared absorption spectra(Fig.3) showing two distinct absorption bands  $\nu_1$  due to tetrahedral (A) site interstitial voids near  $600\text{ cm}^{-1}$  and other  $\nu_2$  due to octahedral (B) site interstitial voids near  $400\text{ cm}^{-1}$ . Our results in this present communication are well supported by previous reports [14, 15].

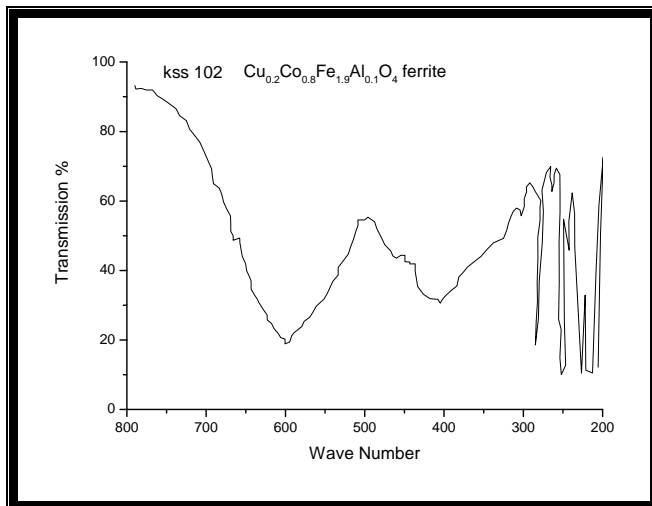


**Figure 3:** IR absorption spectra

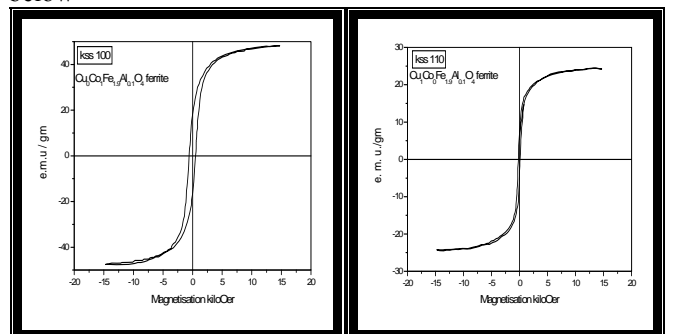
The close inspection of all micrographs (Fig.4) revealed that there is continuous grain growth with well defined grain boundaries formed. The present system shows multi domain behavior.



**Figure 4:** Scanning electron microscope



The hysteresis curves for different samples shown (Fig.5) below



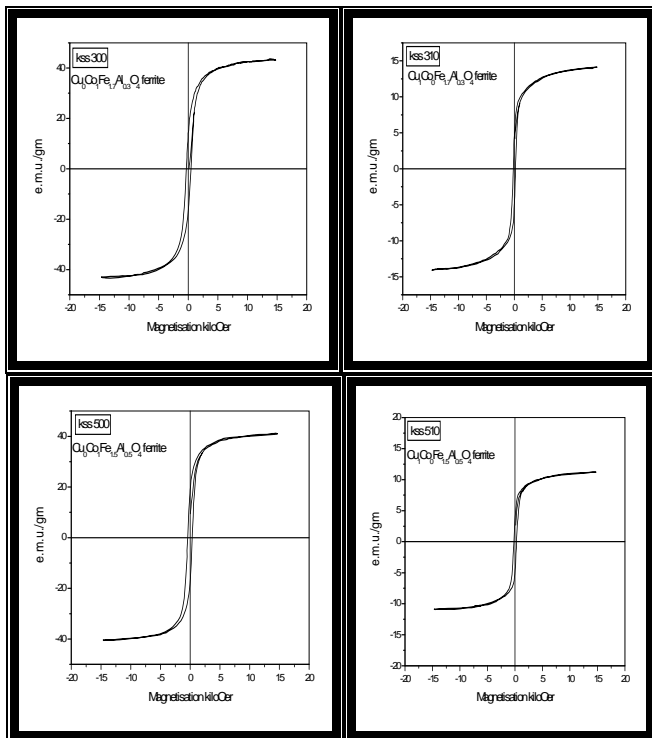


Figure 5: Hysteresis patterns of the samples for  $Cu_xCo_{1-x}Fe_{2-2y}Al_{2y}O_4$  ferrite system

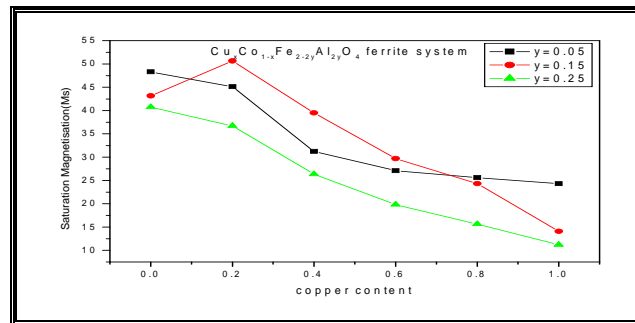


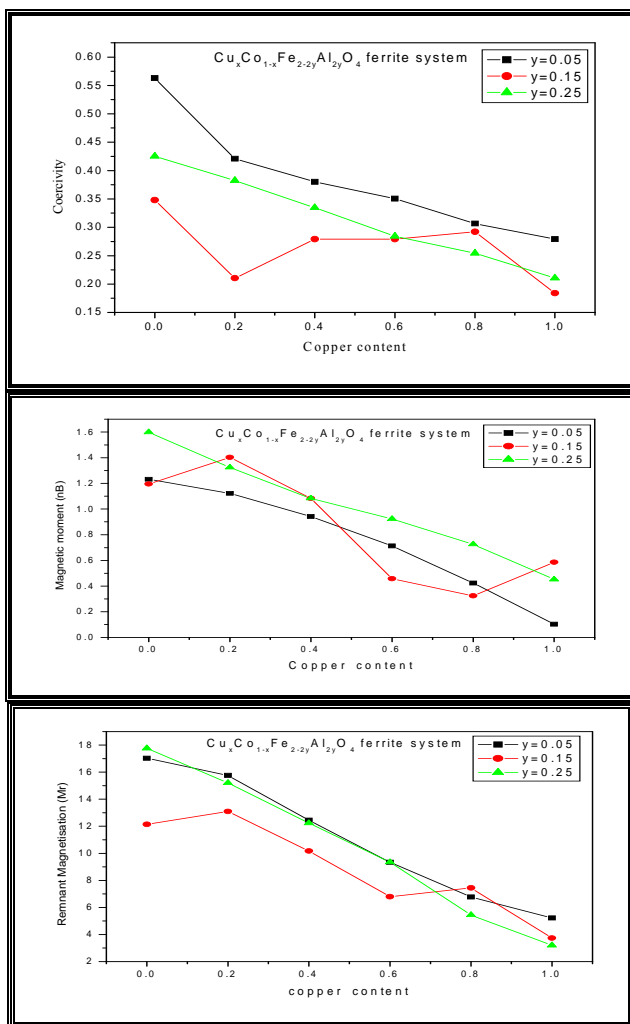
Figure 6: Variation of coercivity, magnetic moment, Remenent magnetization and saturation magnetization with copper and aluminum content for  $Cu_xCo_{1-x}Fe_{2-2y}Al_{2y}O_4$  ferrite system

From figure 6, the value of  $n_B$  was observed which goes on decreasing for aluminum doped copper cobalt ferrite with increasing aluminum and copper content. Addition of  $Cu^{2+}$  content replaces  $Fe^{3+}$  from A to B site which produces canting of the magnetic spins and results in the decrease in both magnetic moments on A and B sites. This clearly indicates the decrease in A-B interaction.

Saturation magnetization is found increasing up to 20 % of copper content and thereafter decreases. The increasing trend of saturation magnetization with  $Cu^{2+}$  content up to  $x=0.2$  suggest that the Neel's two sub - lattice model is predominating up to  $x = 0.2$  and thereafter Y-K three sub lattice predominant. The decrease in saturation magnetization ( $M_s$ ) can also be explained in the light of Yafet-Kittle model of triangular spins.

The coercivity decreases with particle size as suggested by Liu et al. The large value of coercivity essentially originates from the anisotropy of the copper ions at the octahedral (B) site due to its important spin orbit coupling. The coercive field ( $H_c$ ) in Al doped copper cobalt ferrite is found to decrease with increasing Aluminum content in the doped copper cobalt ferrites, which may be attributed to the loss of anisotropy due to the migration of  $Cu^{2+}$  ions to the tetrahedral site and also due to the decrease in the ferrous content in doped copper cobalt ferrite. The decrease in coercivity of samples is accompanied by the reduction of saturation magnetization and remnant magnetization. The reason for the decrease in coercivity of copper cobalt ferrite is the decrease in magneto-crystalline anisotropy by lowering the concentration of  $Fe^{2+}$  ions at the octahedral sites in the spinel lattice because  $Fe^{2+}$  ions are also a source of the magnetic anisotropy in ferrites.

The remnant magnetization ( $M_r$ ) of  $Al^{3+}$  doped copper cobalt ferrite shows a decreasing behavior with increase in copper and  $Al^{3+}$  content from  $x = 0.00$  to  $x = 0.1$  and  $y=0.05, 0.15, 0.25$ . The decrease in  $M_r$  is due to lower magnetic moment of  $Al^{3+}$  as compared to  $Fe^{3+}$ .



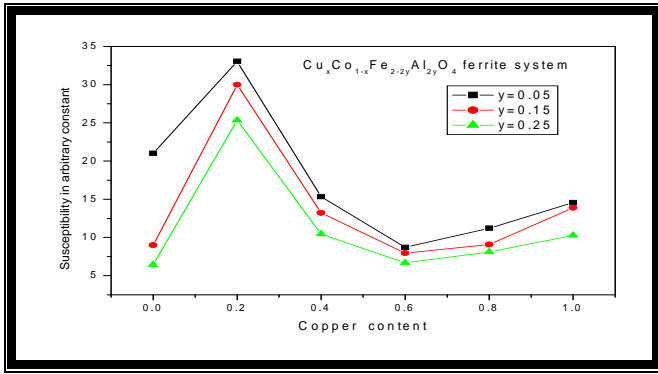


Figure 7 (a): Variation of A. C. susceptibility with copper and aluminium content at room temperature

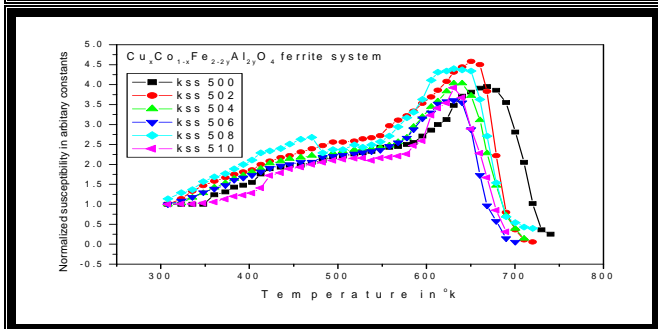
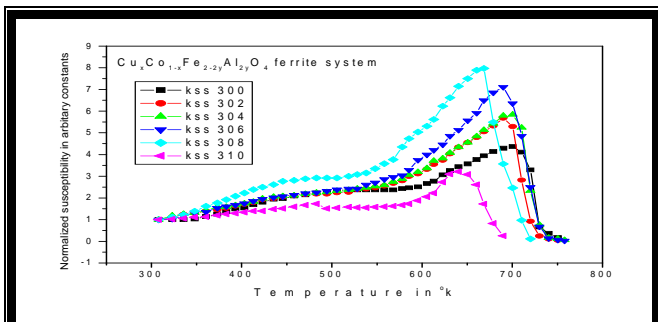
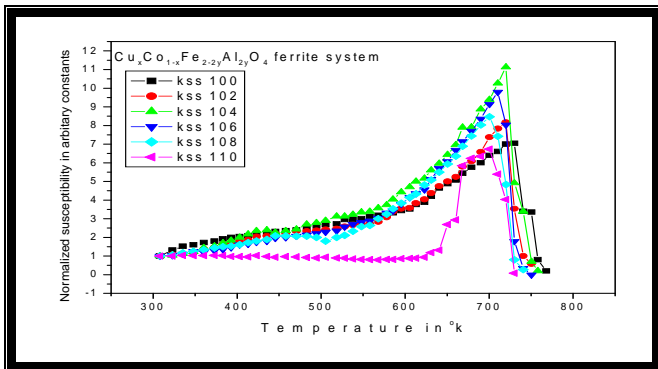


Figure 7 (b): Variation of A. C. susceptibility with copper and aluminium content at various temperatures for  $Cu_xCo_{1-x}Fe_{2-2y}Al_{2y}O_4$  ferrite system

The susceptibility is measured at room temperature then susceptibility is found increasing up to 20 % of copper content and thereafter decreases [Fig.7(a)]. The susceptibility is measured at various temperature [Fig.7(b)], the compositions was shown gradual decrease in normalized susceptibility with temperature suggest that they exhibit super paramagnetic (SP) structure having fine particles. The

susceptibility is decreases and Curie temperature also shifts towards minimum value as copper as well as aluminum content increases.

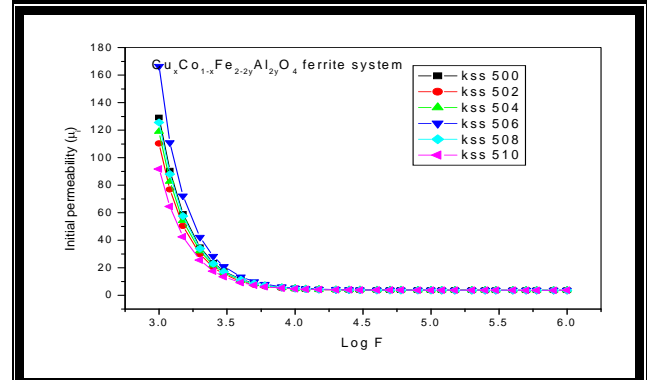
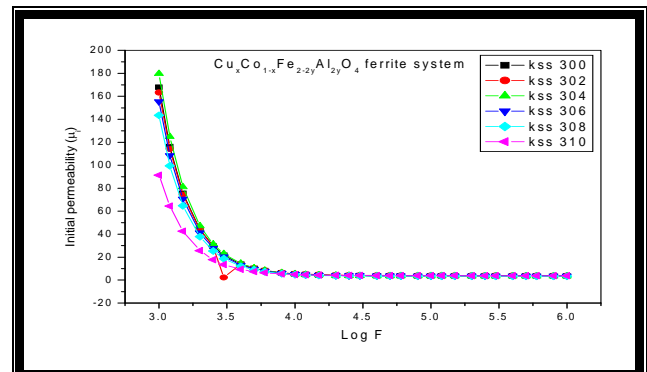
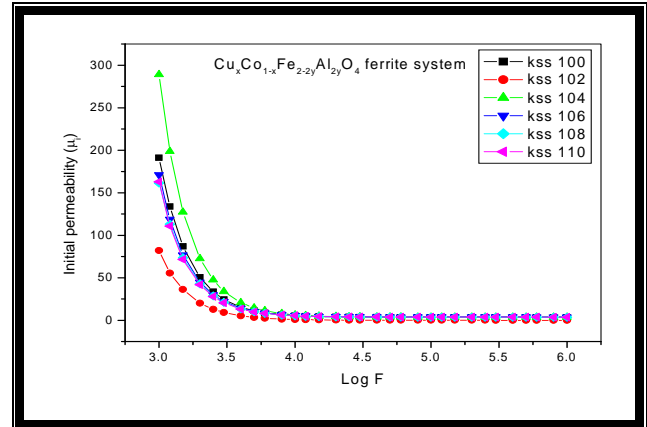


Figure 8: Variation of initial permeability with frequency for  $Cu_xCo_{1-x}Fe_{2-2y}Al_{2y}O_4$  ferrite system

The variation of initial permeability as a function of frequency depicts the dispersion of initial permeability up to 1 KHz and beyond that it remains frequency independent. This low frequency dispersion in  $\mu_i$  is attributed to domain wall displacement. The absence of low frequency resonance indicates that there is no domain wall motion. Thus, the low frequency dispersion in the ferrite compositions is only due to domain wall displacement. Initial permeability decreases with increases the copper content as well as aluminum content (Fig.8).

Figure 9 shows, variation of e.m.u with temperature and from this graph calculated the curie temperature. From the figure 10, it is found that Curie temperature of the compositions goes on decreases with increase in copper as well as aluminum content. It was rather expected because addition of copper replaces  $Fe^{3+}$  to B-site which reduces the

population of  $Fe^{3+}$  on A-site and hence A-site becomes magnetically weak, results in the decrease in A-B interaction. The Curie temperatures are determined by drawing tangent to the paramagnetic tail on the temperature axis. Similar type of paramagnetic tail and Curie temperatures determination has been reported [16, 17].

Curie temperature is the peculiar character of the ferromagnetic / ferri-magnetic materials. Curie temperature is the temperature at which it undergoes the phase transition from Ferro / Ferri-magnetic to paramagnetic state. The magnetic material shows spontaneous magnetization below its Curie point and no magnetization above the Curie temperature. In ferrites, Curie temperature is proportional to number of active magnetic linkages. It is affected by A-B distance and A-O-B angle. A-B interaction depends upon these distances. As these distance increases, Curie temperature decrease as suggested by Gorter and Neel [18-19] Curie temperature depends upon the  $Fe^{3+}$  ions participating in A-B interaction. When  $Fe^{3+}$  ions concentration per molecular formula unit is decreased, then Curie temperature decreased. The behaviour of Curie temperature in aluminium doped copper cobalt ferrite found decrease with concentration of aluminium content indicating the reduction in ferri-magnetic behaviour.

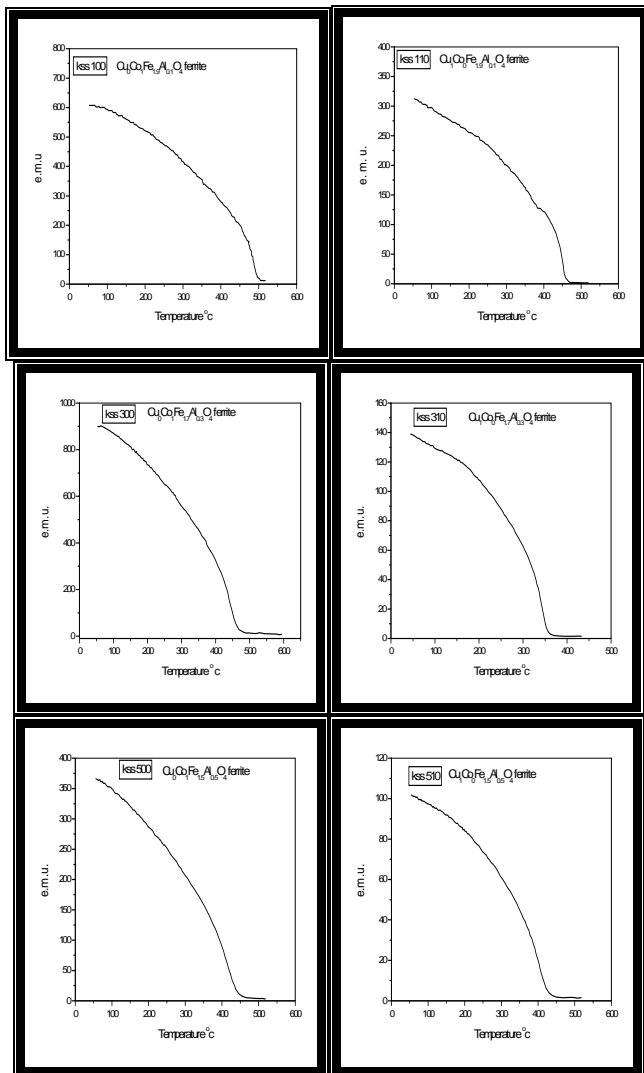


Figure 9: The curie temperatures for  $Cu_xCo_{1-x}Fe_{2-2y}Al_{2y}O_4$  ferrite system

#### 4. Conclusion

Copper cobalt ferrite is partially inverse cubic spinel ferrite. Addition of  $Al^{3+}$  ions replaces  $Fe^{3+}$  on (B) site resulting in increase of lattice constant  $a$ , decrease in ionic radii ( $R_A$ ) and bond length (O-A). The lattice constant obtained from XRD data shows non-linear behaviour. The coercivity ( $H_c$ ), magnetic moment ( $n_B$ ), Remenent magnetization ( $Mr$ ) and saturation magnetization ( $Ms$ ) with copper and aluminum content goes on decreasing. The initial permeability decreases with increase in frequency. The A. C. susceptibility goes on decreasing with copper and aluminum content. The Curie temperature of copper cobalt ferrite decreases with aluminum content.

#### 5. Future Scope

In this communication our aim was to study the effect of Aluminum on electric and magnetic properties of mixed Copper-Cobalt ferrite. Micro-structure of ferrites depends up on preparation technique. There is a scope to reduce the particle size by adopting a preparation technique like wet chemical precipitation method, sol-gel method etc and see the interesting results.

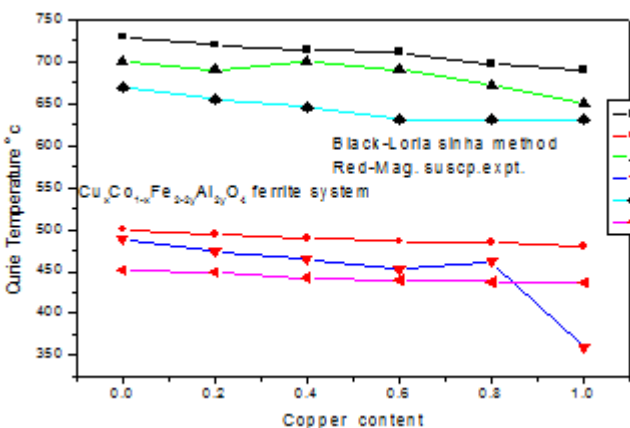


Figure 10: Variation of curie temperature with copper and aluminium content for  $Cu_xCo_{1-x}Fe_{2-2y}Al_{2y}O_4$  ferrite system

#### References

- [1] R. S. Devan, S. A. Lokare, S. S. Chougule, D. R. Patil, Y. D. Kolekar, and B. K. Chougule, J. Phys. Chem. Solids 67, 1524 (2006).
- [2] K. Zhao, K. Chen, Y. R. Dai, J. G. Wan, and J. S. Zhu, Appl. Phys. Lett. 87, 162901 (2005).
- [3] S. R. Kulkarni, C. M. Kanamadi, and B. K. Chougule, Mater. Res. Bull. 40, 2064 (2005)
- [4] Zhao L, Yang H, Yu L, Cui Y, Zhao X, Zou B, Feng SJ. MagnMagn Mater2006;301:445-51.
- [5] Rath C, Sahu KK, Anand S, Date SK, Mishra NC, Das RP. J MagnMagn Mater 1999;202:77-84.
- [6] Rajendran M, Pullar RC, Bhattacharya AK, Das D, Chintalapudi SN, Majumdar CK. J MagnMagn Mater 2001;232:71-83.
- [7] Ozaki M. Mater Res Bull 1989;12:35-43.

- [8] Costa ACM, Tortella E, Morelli MR, Kaufman M, Kiminami RHGA. *J Mater Sci*2002;37:3569–72.
- [9] M.M. Mallapur, B.K. Chougule; *Materials Letters*; Vol. 64 (2010); P. 231–234.
- [10] C. Radhakrishnamurty, S. D. Likhite and N. D. Sastry, *Phil. Mag.*23 (1971) 503.
- [11] H. P. Klug, L. E. Alexander, *X-ray diffraction procedure for polycrystalline and amorphous materials*, (Wiley N.Y 1997)637.
- [12] A. T. Raghavender, R. G. Kulkarni and K.M. Jadhav; *Chinese J. of Phys.*vol.48 No.4 (2010) 512-522.
- [13] A. B. Gadkari, T. J. Shinde, P. N. Vasambekar, *J. Mater Sci: Mater Electron* 21 (2010) 96-103.
- [14] Waldron R.D, *Phy.Rev*; 99(6) (1955)1727.
- [15] A.T. Raghvendra et al. *magn. Mater.* 316 (2007) 1
- [16] Karche B. R, Khasbardar B.V., and Vaingankar A. S., *J. Mag. and Mag. Mater.*168 (1997) 292.
- [17] Naik A.B., Sawant S.R., Patil S.A., and Pawar J.I., *Bull. Mater. Sci.*, 12 (3)(1989)1.
- [18] Gorter E.W., *Saturation magnetization of ferrites with spinel structure*, *Nature*, 165(1950)789.
- [19] Neel L., *Ann. Phy.*, 3(1948)137.